

CHAPTER 2

Topological Properties of Skeletal Structures

2.1 INTRODUCTION

In the analysis of skeletal structures, three different properties are encountered, which can be classified as topological, geometrical and material. Separate study of these properties results in a considerable simplification in the analysis and leads to a clear understanding of the structural behaviour. This chapter is confined to partial study of the topological properties of skeletal structures, since both displacement and force methods require such a study at the beginning of the analysis. The number of equations to be solved in the two methods may differ widely for the same structure. This number depends on the size of flexibility and stiffness matrices, which are the same as the degree of statical indeterminacy (DSI) and the degree of kinematical indeterminacy (DKI) of a structure, respectively. Obviously, the method which leads to the required results with the least amount of effort, should be used for the analysis of a given structure. Thus, the comparison of the numbers of DSI and DKI may be the main deciding criterion for selecting the method of analysis.

For determining the DSI and DKI of structures, numerous formulae, depending on the kinds of member or types of joint, have been given, e.g. Refs [38,200,236]. The use of these classical formulae, in general, requires counting the number of members and joints, which becomes a tedious process for multi-member and/or complex pattern structures. This counting process provides no additional information about their connectivity properties.

Henderson and Bickley [77] related the DSI of a rigid-jointed frame to the first Betti number (cyclomatic number) of its graph model S . This was an important

achievement, since a topological invariant of a graph was related to an essential mechanical property of the corresponding structure. Generalizing the Betti's number to a linear function and using an expansion process, Kaveh [89] developed a general method for determining the DSI and DKI of all types of skeletal structures. Special methods have also been developed to transform the topological properties of space structures to those of their planar drawings to simplify the calculation of their DSI, Refs [90,91,109].

In this chapter, general and simple methods are presented for calculating the DSI and DKI of different types of skeletal structures, such as rigid-jointed planar and space frames, pin-jointed planar trusses and ball-jointed space trusses. Euler's polyhedra formula is then used to develop very efficient special methods for determining the DSI of different types of structures. An automatic algorithm is presented for efficient planar embedding of structural models.

2.2 MATHEMATICAL MODEL OF A SKELETAL STRUCTURE

The mathematical model S of a structure is considered to be a finite, connected graph. There is a one-to-one correspondence between the elements of the structure and the members of S . There is also a one-to-one correspondence between the joints and the nodes of S , except for the support joints. Two different groups of modelling are considered. The first group is suitable for calculating the DSI and DKI of structures, and the second group is more appropriate for analysis. These models are illustrated in Figure 2.1.

For a frame structure, all the support joints are identified as a datum (ground) node in the first group of model, Figures 2.1(b1) and (b2). In the second group, all such joints are connected by an artificial tree, Figures 2.1 (c1) and (c2).

Truss structures are assumed to be supported in a statically determinate fashion (Figures 2.1 (b3) and (b4)), and the effect of additional supports can easily be included in calculating the DSI and DKI of the corresponding structures. In the second group of models, artificial members are added as shown in Figures 2.1 (c3) and (c4). For a fixed support, two members and three members are considered for planar and space trusses, respectively, and one member is used for representing a roller.

The skeletal structures are considered to be in perfect condition; i.e. planar and space trusses have pin and ball joints only. Obviously the effect of extra constraints or releases can easily be taken into account in determining their DSI and DKI, and also in their analysis, Mauch and Fenves [168].

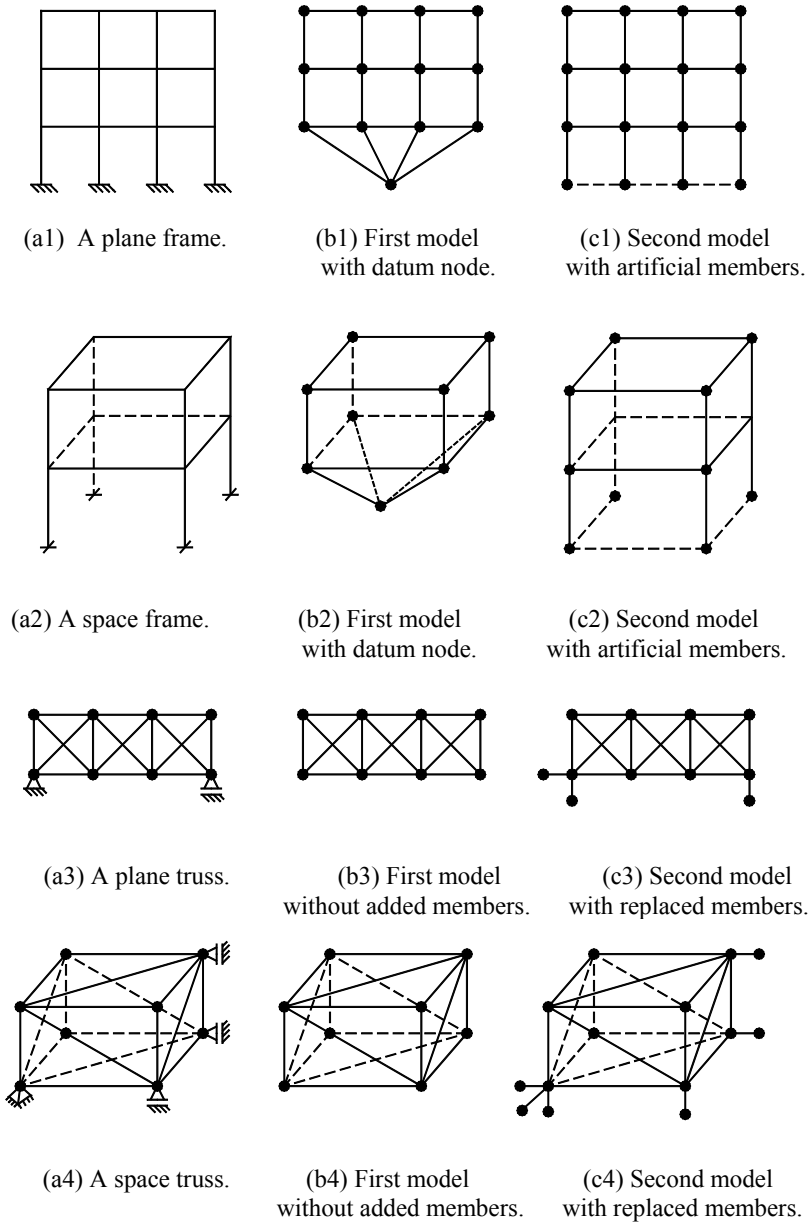


Fig. 2.1 Different types of skeletal structures with their models.

2.3 UNION-INTERSECTION METHOD

The degree of kinematical indeterminacy of a structure is the number of independent displacement components (translations and rotations) required for describing a general deformation state of the structure. The DKI is also referred to as the total degrees of freedom of the structure. On the other hand, the degree of statical indeterminacy (redundancy) of a structure is the number of independent force components (forces and moments) required for describing a general equilibrium state of the structure. The DSI of a structure can be obtained by reducing the number of independent equilibrium equations from the number of its unknown forces.

Formulae for calculating the DKI and DSI of various skeletal structures can be found in text books on structural mechanics, e.g. for planar trusses each joint of which has two degrees of freedom, the DKI, denoted by $\eta(S)$, is given as,

$$\eta(S) = 2N(S) - 3, \quad (2-1)$$

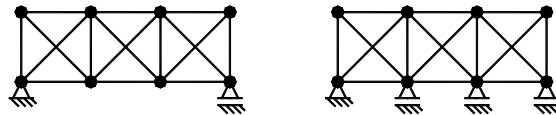
where S is supported in a statically determinate fashion. For extra support, $\eta(S)$ will further be reduced by one for each additional constraint.

As an example, for the trusses shown in Figures 2.2(a) and 2(b), the DKIs are obtained as $\eta(S) = 2 \times 8 - 3 = 13$ and $\eta(S') = 2 \times 8 - 5 = 11$, respectively.

The DSI of a planar truss, denoted by $\gamma(S)$, can be calculated from,

$$\gamma(S) = M(S) - 2N(S) + 3, \quad (2-2)$$

where S is supported in a statically determinate fashion (internal indeterminacy). For extra supports (external indeterminacy), $\gamma(S)$ should be further increased by the number of additional unknown reactions. As an example, for the trusses shown in Figures 2.2(a) and 2(b), the DSIs are calculated as $\gamma(S) = 16 - 2 \times 8 + 3 = 3$ and $\gamma(S') = 16 - 2 \times 8 + 5 = 5$, respectively.



(a) Statically determinate supported truss S. (b) Truss S' with additional supports.

Fig. 2.2 Planar trusses.

Similar formulae are derived for space trusses:

$$\eta(S) = 3N(S) - 6, \quad (2-3)$$

$$\gamma(S) = M(S) - 3N(S) + 6. \quad (2-4)$$

For the space truss of Figure 2.1(a4), these values are $\eta(S) = 3 \times 8 - 6 = 18$ and $\gamma(S) = 18 - 3 \times 8 + 6 = 0$.

For planar and space frames, the classical formulae are given as,

$$\eta(S) = \alpha [N(S) - 1], \quad (2-5)$$

$$\gamma(S) = \alpha [M(S) - N(S) + 1], \quad (2-6)$$

where all supports are modelled as a datum (ground) node, and $\alpha = 3$ or 6 for planar and space frames, respectively. As an example, $\eta(S)$ and $\gamma(S)$ are calculated for the planar and space frames shown in Figures 2.1(b1) and (b2). For the planar frame $\eta(S) = 3(13 - 1) = 36$ and $\gamma(S) = 3(21 - 13 + 1) = 27$, and for the space frame $\eta(S) = 6(9 - 1) = 48$ and $\gamma(S) = 6(16 - 9 + 1) = 48$.

All these formulae require counting a great number of members and nodes, which makes their application impractical for multi-member and complex pattern structures.

2.3.1 A UNIFYING FUNCTION

All the existing formulae for determining the DKI and DSI have a common property, which is their linearity with respect to $M(S)$ and $N(S)$. Therefore, a general unifying function is,

$$v(S) = aM(S) + bN(S) + cv_0(S), \quad (2-7)$$

where $M(S)$, $N(S)$ and $v_0(S)$ are the numbers of members, nodes and components of S , respectively. The coefficients a , b and c are integer numbers depending on both the type of the corresponding structure and the property which the function is expected to represent. For example, $v(S)$ with appropriate values for a , b and c may describe the DKI or DSI of certain types of skeletal structures, Table 2.1. For $a = 1$, $b = -1$ and $c = 1$, $v(S)$ becomes the first Betti number $b_1(S)$ of S .

Table 2.1 The coefficient for the classical formulae.

Type of structure	v(S)	a	b	c
Plane frame	DKI	0	+3	-3
	DSI	+3	-3	+3
Space frame	DKI	0	+6	-6
	DSI	+6	-6	+6
Plane truss	DKI	0	+2	-3
	DSI	+1	-2	+3
Space truss	DKI	0	+3	-6
	DSI	+1	-3	+6

It should be noted the $v(S)$ can further be generalized to include the effect of higher order elements. As an example, when a skeletal structure contains shear panels then one may use,

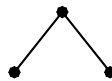
$$v(S) = dV(S) + aM(S) + bN(S) + cv_0(S),$$

where $V(S)$ is the number of shear panels of the structure, and d is an integer.

2.3.2 AN EXPANSION PROCESS

An expansion process in its simplest form has been used for re-forming structural models such as simple planar and space trusses, Müller-Breslau [176]. A simple planar truss can be formed by the following expansion process:

Consider a subgraph S_0 with two members connected at a node as shown in Figure 2.3(a). Start with a member and join a typical S_0 so that their intersection contains two disjoint nodes, Figure 2.3(b). Continue this process joining another S_0 to the previously formed subgraph, until the whole truss is formed. Such a graph is the model of a simple planar truss.



(a) A typical subgraph S_0 .

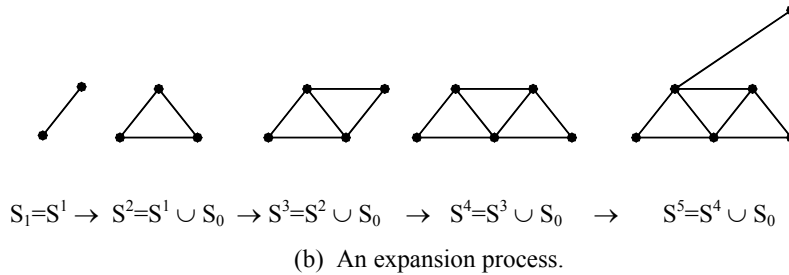
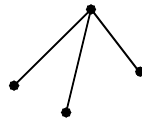


Fig. 2.3 Formation of a planar simple truss.

Similarly, a simple space truss can be re-formed by joining a subgraph S_0 containing three members connected at a node, which are not in a plane, to a triangle to form a tetrahedron, Figure 2.4. This process should be continued to obtain the entire truss. At each stage of expansion, the intersection consists of three disjoint nodes.



(a) A typical subgraph S_0 .

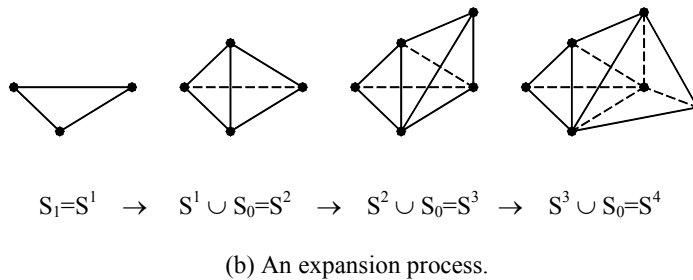


Fig. 2.4 Formation of a simple space truss.

In the above expansion process, the properties of S_0 , and the way this typical subgraph is joined to the previously expanded subgraph, guarantee the determinacy of the simple truss.

The idea can be extended to other types of structure. As an example, a tree-shaped frame can be re-formed by adding one member at each stage of an expansion as shown in Figure 2.5.

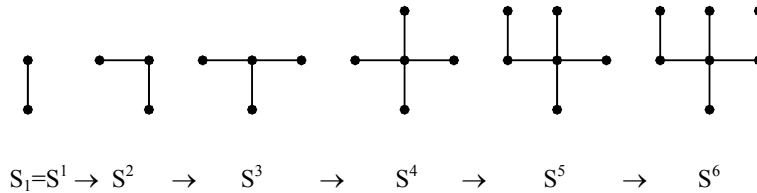


Fig. 2.5 Formation of a tree-shaped frame model.

2.3.3 AN INTERSECTION THEOREM

In a general expansion process, a subgraph S_i may be joined to another subgraph S_j in an arbitrary manner. For example $\gamma(S_i)$ or $\gamma(S_j)$ may have any arbitrary values and the union $S_i \cup S_j$ may be a connected or a disjoint subgraph. The intersection $S_i \cap S_j$ may also be connected or disjoint. It is important to find the properties of $S_i \cup S_j$, having the properties of S_i , S_j and $S_i \cap S_j$. However, one cannot simply employ an additivity formula of the following form,

$$v(S_i \cup S_j) = v(S_i) + v(S_j) - v(S_i \cap S_j),$$

as is often thought. As an example, consider a planar truss containing S_1 and S_2 as its subgraphs, Figure 2.6. In order to calculate the DSI of S by,

$$\gamma(S) = M(S) - 2N(S) + 3\gamma_0(S),$$

we have, $\gamma(S_1) = 5 - 2 \times 4 + 3 = 0, \quad \gamma(S_2) = 1 - 2 \times 2 + 3 = 0,$

and $\gamma(S_1 \cap S_2) = 0 - 2 \times 2 + 3 \times 2 = 2,$

leading to, $\gamma(S_1 \cup S_2) = 0 + 0 - (2) = -2,$

which is an incorrect answer. However, if $\gamma(S_1 \cap S_2)$ is replaced by $\bar{\gamma}(S_1 \cap S_2) = M(S) - 2N(S) + 3$, then the correct result will be obtained.

$$\bar{\gamma}(S_1 \cap S_2) = 0 - 2 \times 2 + 3 = -1,$$

leading to: $\gamma(S_1 \cup S_2) = 0 + 0 - (-1) = +1.$

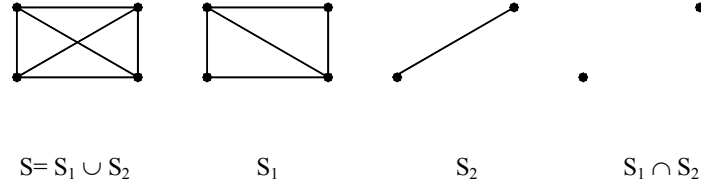


Fig. 2.6 A truss, its subgraphs and their intersections.

The relationship given in the above becomes totally wrong if S_i and/or S_j contain more than one component. The following theorem removes all the difficulties and leads to a correct calculation of the properties of $S_i \cup S_j$. In order to have the formula in its general form, q subgraphs are considered in place of two subgraphs.

Theorem (Kaveh [89]): Let S be the union of q subgraphs $S_1, S_2, S_3, \dots, S_q$ with the following functions being defined:

$$v(S) = aM(S) + bN(S) + cv_0(S),$$

$$v(S_i) = aM(S_i) + bN(S_i) + cv_0(S_i) \quad i = 1, 2, \dots, q$$

$$v(A_i) = aM(A_i) + bN(A_i) + cv_0(A_i) \quad i = 2, 3, \dots, q,$$

where $A_i = S^{i-1} \cap S_i$ and $S^{i-1} = S_1 \cup S_2 \cup \dots \cup S_{i-1}$. Then:

$$[v(S) - cv_0(S)] = \sum_{i=1}^q [v(S_i) - cv_0(S_i)] - \sum_{i=2}^q [v(A_i) - cv_0(A_i)]. \quad (2-8)$$

Proof: According to Eq. (2-7):

$$\begin{aligned}
 v(S) = aM(S) + bN(S) + cv_0(S) &= a \{M(S_1) + \sum_{i=2}^q [M(S_i) - M(A_i)]\} + b \{N(S_1) \\
 &+ \sum_{i=2}^q [N(S_i) - N(A_i)]\} + cv_0(S).
 \end{aligned}$$

Adding,

$$[c \sum_{i=1}^q v_0(S_i) - c \sum_{i=1}^q v_0(S_i)] + [c \sum_{i=2}^q v_0(A_i) - c \sum_{i=2}^q v_0(A_i)] = 0,$$

and rearranging the terms, the proof is completed as follows:

$$\begin{aligned}
[v(S) - cv_0(S)] &= \sum_{i=1}^q [aM(S_i) + bN(S_i) + cv_0(S_i)] \\
&- \sum_{i=2}^q [aM(A_i) + bN(A_i) + cv_0(A_i)] - c \sum_{i=1}^q v_0(S_i) + c \sum_{i=2}^q v_0(A_i) \\
&= \sum_{i=1}^q [v(S_i) - cv_0(S_i)] - \sum_{i=2}^q [v(A_i) - cv_0(A_i)].
\end{aligned}$$

Special Case: If S and each of its subgraphs considered for expansion (S_i for $i = 1, \dots, q$) are non-disjoint (connected), then Eq. (2-8) can be simplified as,

$$v(S) = \sum_{i=1}^q v(S_i) - \sum_{i=2}^q \bar{v}(A_i), \quad (2-9)$$

where:

$$\bar{v}(A_i) = aM(A_i) + bN(A_i) + c.$$

For calculating the DKI and DSI of a complex structure or a structure with a large number of members, one normally selects a repeated unit of the structure and joins these units sequentially in a connected form. Thus, Eq. (2-9) can be applied in place of Eq. (2-8) to obtain the overall property of the structure.

2.3.4 A METHOD FOR DETERMINING THE DKI AND DSI OF STRUCTURES

Let S be the union of its repeated and/or simple pattern subgraphs S_i ($i=1, \dots, q$). Calculate the DKI or DSI of each subgraph using the appropriate coefficients from Table 2.1. Now perform the following steps:

Step 1. Join S_1 to S_2 to form $S^2 = S_1 \cup S_2$, and calculate the DKI or DSI of their intersection $A_2 = S_1 \cap S_2$. The value of $v(S^2)$ can be found using Eq. (2-8) or Eq. (2-9), as appropriate.

Step 2. Join S_3 to S^2 to obtain $S^3 = S^2 \cup S_3$, and determine the DKI or DSI of $A_3 = S^2 \cap S_3$. Similarly to Step 1, calculate $v(S^3)$.

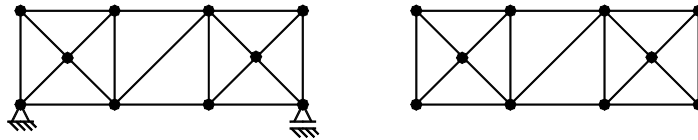
Step k . Subsequently join S_{k+1} to S^k , calculating the DKI or DSI of $A_{k+1} = S^k \cap S_{k+1}$ and evaluating the magnitude of $v(S^{k+1})$.

Repeat Step k until the entire structural model $S = \bigcup_{i=1}^q S_i$ is reformed and its DKI or DSI is determined.

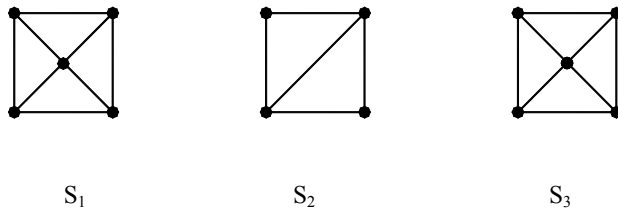
In the above expansion process, the value of q depends on the properties of the substructures (subgraphs) which are considered for reforming S. These subgraphs have either simple patterns for which $v(S_i)$ can easily be calculated, or the value of their DKI or DSI are already known.

In the process of expansion, if an intersection A_i itself has a complex pattern, further refinement is also possible; i.e. the intersection can be considered as the union of simpler subgraphs.

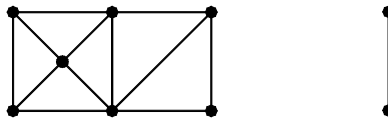
Example 1: A simple structure S is chosen to illustrate the steps and capabilities of the method, as shown in Figure 2.7(b). The union and intersections at each step are depicted in Figures 2.7(c) and (d). The crossing points at the first and third panels are also considered as extra nodes.



(a) A skeletal structure and its graph model.

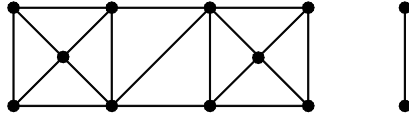


(b) Subgraphs of S.



$S_1 \cup S_2$ $A_2 = S_1 \cap S_2$

(c) The union and intersection of S_1 and S_2 .



$S^2 \cup S_3$ $A_3 = S^2 \cap S_3$

(d) The union and intersection of S^2 and S_3 .

Fig. 2.7 An expansion process for reforming S .

When S is viewed as a planar truss supported in a statically determinate fashion, then using Eq. (2-2) for calculating DSIs of S_i and A_i , we obtain,

$$\gamma(S^2) = \gamma(S_1 \cup S_2) = (1)+(0) - (1-4+3) = 1,$$

and performing the second step leads to:

$$\gamma(S^3) = \gamma(S) = \gamma(S^2 \cup S_3) = (1)+(1) - (1-4+3) = 2.$$

The DKI for this truss is obtained in a similar manner using Eq. (2-1) for calculating the DKI of subgraphs and their intersections, and considering the support conditions, we obtain:

$$\eta(S_1) = 2N(S_1) - 2 = 10 - 2 = 8, \quad \eta(S_2) = 2N(S_2) = 8,$$

$$\eta(S_3) = 2N(S_3) - 1 = 10 - 1 = 9, \quad \eta(A_2) = 2 \times 2 = 4, \quad \text{and} \quad \eta(A_3) = 2 \times 2 = 4.$$

Therefore:

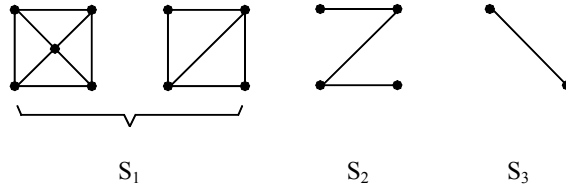
$$\eta(S^2) = (8)+(8) - (4) = 12 \quad \text{and} \quad \eta(S^3) = \eta(S) = (12)+(9) - (4) = 17.$$

For S as the graph model of a rigid-jointed frame, Eqs (2-5) and (2-6) are used and the following results are obtained:

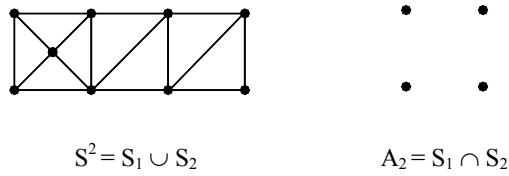
$$\text{For the plane frame} \quad \gamma(S) = 30, \quad \eta(S) = 27,$$

$$\text{and for the plane truss} \quad \gamma(S) = 2, \quad \eta(S) = 17.$$

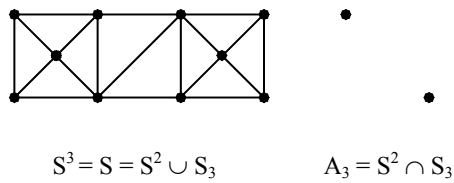
An expansion process using different decomposition of S is also considered. In this case, S is decomposed into three subgraphs, as shown in Figure 2.8(a), and Eq. (2-8) is used in place of Eq. (2-9), since S_1 is a disjoint subgraph. The expansion process is illustrated in Figure 2.8.



(a) Selected subgraphs of S .



(b) Operation of the first step.



(c) Operation of the second step.

Fig. 2.8 A different decomposition of S .

When S is viewed as a truss, using appropriate coefficients from Table 2.1, using Eq. (2-8) results in

$$[\gamma(S^2) - 3] = [1 - 3 \times 2] + [-2 - 3 \times 1] - [4 - 3 \times 4],$$

or $\gamma(S^2) = 1.$

Similarly for the second step,

$$[\gamma(S^3) - 3] = [1 - 3 \times 1] + [0 - 3 \times 1] - [-4 + 6 - 3 \times 2],$$

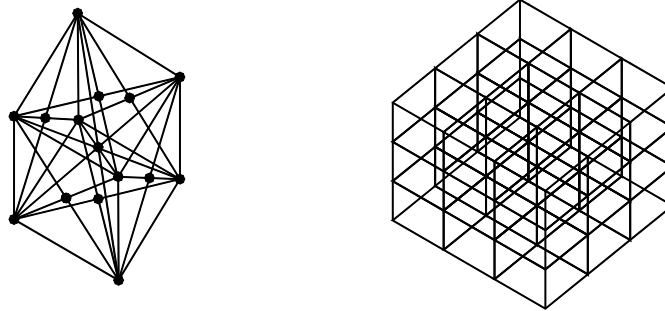
or
$$\gamma(S^3) = \gamma(S) = 2.$$

In order to calculate the DKI, Eq. (2-7) is used for determining the DKIs of the subgraphs and intersections (with appropriate coefficients from Table 2.1), and the same results as the previous ones are obtained.

Example: Let S be the graph model of a space structure. This graph can be considered as 27 subgraphs S_i as shown in Figure 2.9(a), connected to each other to form a graph $S = \bigcup_{i=1}^{27} S_i$. The interfaces of S_i ($i=1, \dots, 27$) are shown in Figure 2.9(b), in which some of the members are omitted for the sake of clarity.

The expansion process consists of joining 27 subgraphs S_i one at a time. In this process, the selected subgraphs can have three different types of intersections, which are shown in Figure 2.10(a).

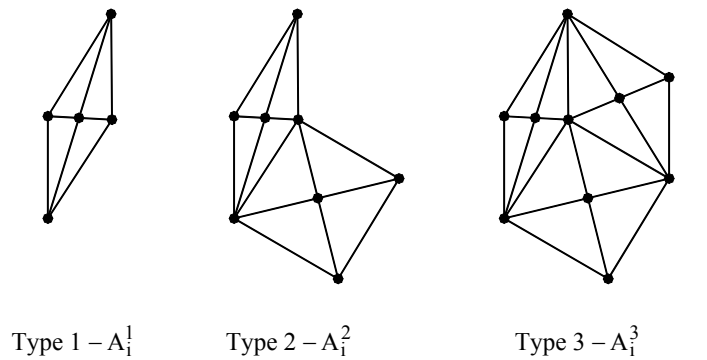
In order to simplify the counting and the recognition of the types of interface, S is re-formed storey by storey. For the first storey, a 3×3 table is constructed to show the types of intersection occurring in the process of expansion. The numbers on each box designate the type of intersection, Figure 2.10(b). Similar tables are used for the second storey and the third storey of S , Figure 2.10(b).



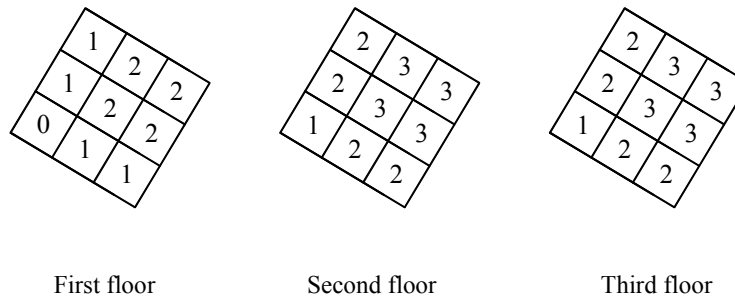
(a) A subgraph S_i of S . (b) $S = \bigcup_{i=1}^{27} S_i$ without some of its members.

Fig. 2.9 A space structure S .

Thus there exist 6 intersections of type A_i^1 , 12 intersections of type A_i^2 and 8 intersections of type A_i^3 .



(a) Three different types of intersection.



(b) Types of intersection after the completion of each storey.

Fig. 2.10 Intersections and their types.

Since each S_i is a connected subgraph, and in the process of expansion, S_i is kept connected, a simplified Eq. (2-8) can be employed:

$$v(S) = \sum_{i=1}^{27} v(S_i) - \sum_{i=2}^{27} \bar{v}(A_i).$$

As has been shown:

$$\sum_{i=2}^{27} \bar{v}(A_i) = \sum_{i=2}^7 \bar{v}(A_i^1) + \sum_{i=8}^{19} \bar{v}(A_i^2) + \sum_{i=20}^{27} \bar{v}(A_i^3).$$

A typical S_i can be considered as,

$$S_i = K_i \cup L_i,$$

where K_i is the 1-skeleton of a fully triangulated cube and L_i is a star connecting the middle node F to the corner nodes of the cube, Figure 2.11. Thus:

$$v(S_i) = v(K_i) + v(L_i) - \bar{v}(K_i \cap L_i).$$

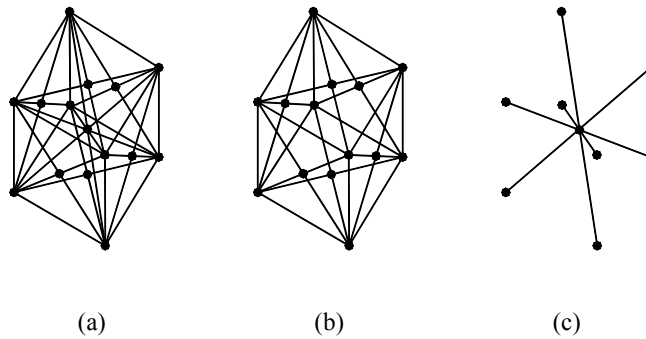


Fig. 2.11 Decomposition of $S_i = K_i \cup L_i$.

Similarly, A_i^2 and A_i^3 can be decomposed as:

$$A_i^2 = A_i^1 \cup A_i^1 \quad \text{and} \quad A_i^3 = A_i^2 \cup A_i^1.$$

When S is viewed as a ball-jointed truss, the DSI of S can be calculated as follows:

$$\gamma(S_i) = (0) + (8 - 3 \times 9 + 6) - (0 - 3 \times 8 + 6) = +5.$$

A simple reason for $\gamma(K_i) = 0$ will be given in Section 2.5.

$$\bar{\gamma}(A_i^1) = M - 3N + 6 = 8 - 3 \times 5 + 6 = -1,$$

$$\bar{\gamma}(A_1^2) = (-1) + (-1) - (1 - 3 \times 2 + 6) = -3,$$

$$\bar{\gamma}(A_1^3) = (-1) + (-3) - (2 - 3 \times 3 + 6) = -3.$$

Hence: $\gamma(S) = 27(5) - [6(-1) + 12(-3) + 8(-3)] = 201.$

When S is taken as a space rigid-jointed frame, then $\gamma(S) = 3564$ is obtained.

Similar calculations are performed for determining the DKI of S, and $\eta(S) = 591$ and $\eta(S) = 1188$ are obtained for ball-jointed truss and space frame, respectively.

The union-intersection method becomes very efficient for structures with repeated patterns. Counting is reduced considerably by this method. As an example, the use of the classical formula for finding the DSI of S in the above example requires counting 792 members and 199 nodes, which is not an easy task with a probable mistake in the process of counting.

2.3.5 MODIFICATIONS ON A STRUCTURE

For design of a structure, it is sometimes necessary to add or delete a node, a member or a substructure. The effect of such operations on the DKI or DSI of a structure can easily be found using the intersection theorem.

Example: Suppose a member m_k is added in between two existing nodes n_i and n_j of S, as shown in Figure 2.12; i.e. $S_c = S \cup m_k$. From Eq. (2-9):

$$\begin{aligned}\gamma(S_c) &= \gamma(S) + \gamma(m_k) - \bar{\gamma}(S \cap m_k) \\ &= 3 \times 6 + 0 - 3(0 - 2 + 1) = 21.\end{aligned}$$

Similarly, if m_p is deleted from S, i.e. $S_r = S - m_p$, then,

$$\gamma(S) = \gamma(S_r) + \gamma(m_p) - \bar{\gamma}(S_r \cap m_p)$$

or

$$\begin{aligned}\gamma(S_r) &= \gamma(S) - \gamma(m_p) + \bar{\gamma}(S_r \cap m_p) \\ &= 3 \times 6 - (0) + 3(0 - 2 + 1) = 15.\end{aligned}$$

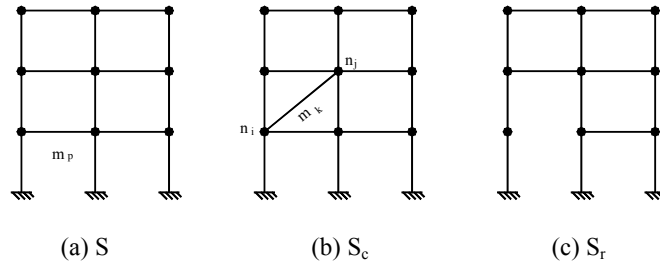


Fig. 2.12 Modifications on a planar frame.

The idea is more general and the effect of adding or deleting a substructure can easily be determined. As an example, consider a planar truss S , as shown in Figure 2.13(a). If a substructure, as illustrated in Figure 2.13(b), is deleted from S , then the reduced S_r (Figure 2.13(c)) is obtained, for which $\gamma(S_r)$ can be calculated using Eq. (2-9) as:

$$\gamma(S) = \gamma(S_r) + \gamma(S_d) - \bar{\gamma}(S_r \cap S_d).$$

Hence:
$$\gamma(S_r) = \gamma(S) - \gamma(S_d) + \bar{\gamma}(S_r \cap S_d) \tag{2-10}$$

$$= (32) - (-2) + (0 - 2 \times 10 + 3) = 17.$$

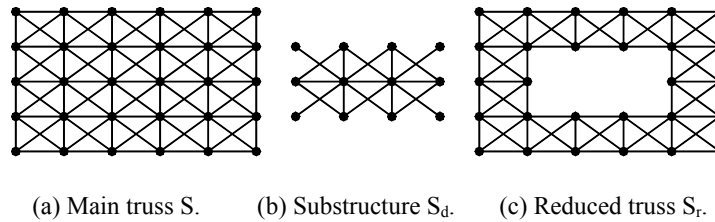


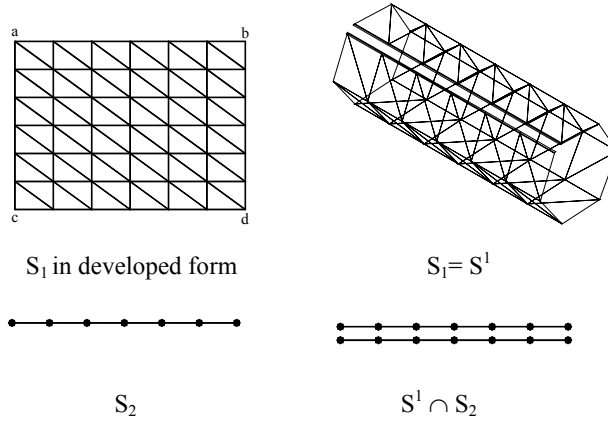
Fig. 2.13 Modifications on a planar truss.

A similar process can be used for determining the DKI for a modified structure.

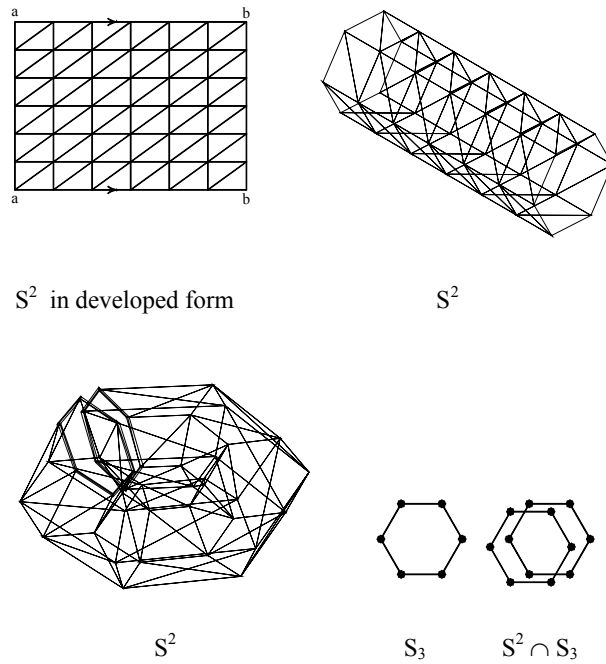
2.4 IDENTIFICATION METHOD

This approach is also based on the union-intersection method and provides a simple means for finding the topological properties of a structural model S , after identifying two subgraphs of S . For example, consider a model as shown in Figure 2.14(a). Identifying ab with cd , as in Figure 2.14(b), results in a cylindrical space

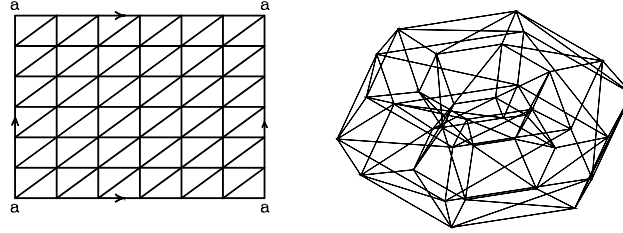
graph S^2 . Identification of ac and bd , leads to a torus-like skeletal structure as depicted in Figure 2.14(c).



(a) S_1 , S_2 and $S^1 \cap S_2$.



(b) S^2 , S_3 and $S^2 \cap S_3$.

(c) A torus-like structure $S^3 = S$.**Fig. 2.14** Identifications in a structure.

The following equation can be employed in such an approach, which is similar to Eq. (2-9) of the previous section.

$$v(S^i \cup S_j) = v(S^i) + v(S_j) - \bar{v}(S^i \cap S_j). \quad (2-11)$$

In this relation, however, S_j is a subgraph of S^i through which the identification has been made. Obviously $S^i \cap S_j$ consists of two disjoint S_j .

Example: Let S_1 be the graph model of a rigid-jointed frame, Figure 2.14(a). The first Betti number of S^3 which is the 1-skeleton of a torus, is obtained by two identifications, as shown in Figures 2.14(b) and (c).

In the case $v(S) = b_1(S) = M(S) - N(S) + b_0(S)$, for the first identification:

$$b_1(S^1) = 72 \quad b_1(S_2) = 0,$$

$$\bar{b}_1(S^1 \cap S_2) = 12 - 14 + 1 = -1,$$

$$b_1(S^1 \cup S_2) = b_1(S^2) = (72) + (0) - (-1) = 73.$$

For the second identification:

$$b_1(S^2) = 73, \quad b_1(S_3) = 1,$$

$$\bar{b}_1(S^2 \cap S_3) = 12 - 12 + 1 = 1,$$

$$b_1(S^2 \cup S_3) = b_1(S^3) = (73) + (1) - (1) = 73.$$

When S is viewed as a space frame, the DSI can easily be found as $\gamma(S) = 6b_1(S) = 6 \times 73 = 438$. For S viewed as a ball-jointed truss, the DSI can be determined as follows:

For the first identification:

$$\gamma(S^1) = M - 3N + 6 = 120 - 3 \times 49 + 6 = -21,$$

$$\gamma(S_2) = 6 - 3 \times 7 + 6 = -9,$$

$$\bar{\gamma}(S^1 \cap S_2) = 12 - 3 \times 14 + 6 = -24,$$

$$\gamma(S^1 \cup S_2) = \gamma(S^2) = (-21) + (-9) - (-24) = -6.$$

For the second identification:

$$\gamma(S^2) = -6, \quad \gamma(S_3) = 6 - 3 \times 6 + 6 = -6,$$

$$\bar{\gamma}(S^2 \cap S_3) = 12 - 3 \times 12 + 6 = -18,$$

$$\gamma(S^2 \cup S_3) = \gamma(S^3) = (-6) + (-6) - (-18) = 6.$$

2.5 THE DSI OF STRUCTURES: SPECIAL METHODS

In this section, using Euler's polyhedra formula (Section 1.8.1), some useful theorems are proven, which provide simple means for calculating the DSI of various types of skeletal structures.

Theorem 1: For a fully triangulated planar truss (except the exterior boundary), the internal DSI is the same as the number of its internal nodes:

$$\gamma(S) = N_i(S). \quad (2-12)$$

Proof: Draw S in the plane. According to Euler's formula,

$$R(S) - M(S) + N(S) = 2, \quad (2-13)$$

where $R(S) = R_i(S) + 1$ is the total number of regions and $R_i(S)$ is the number of triangles. Since all the internal regions are triangles,

$$3R_i(S) = 2M(S) - M_e(S), \quad (2-14)$$

$M_e(S)$ being the number of members in the exterior boundary of S which may be any polygon. Substituting,

$$M_e(S) = N_e(S) = N(S) - N_i(S), \quad (2-15)$$

in Eq. (2-14) leads to:

$$3R_i(S) = 2M(S) - N_e(S) = 2M(S) - N(S) + N_i(S). \quad (2-16)$$

From Eq. (2-13), we have:

$$R_i(S) = M(S) - N(S) + 1. \quad (2-17)$$

Substituting from Eq. (2-17) in Eq. (2-16) yields:

$$M(S) - 2N(S) + 3 = N_i(S).$$

Thus:

$$\gamma(S) = N_i(S).$$

For trusses with non-triangulated internal regions (Figure 2.15(a)), let $M_{ci}(S)$ be the number of members required for completion of the triangulation of the internal regions of S , then:

$$\gamma(S) = N_i(S) - M_{ci}(S). \quad (2-18)$$

The number of members required for triangulation of a polygon is constant and independent of the way it is triangulated. This is why Eq. (2-18) can easily be established.

Once the internal DSI of a structure is found, the external DSI resulting from the additional supports can easily be added, to obtain the total DSI.

Example: For the truss shown in Figure 2.13(a), the application of Eq. (2-12) results in:

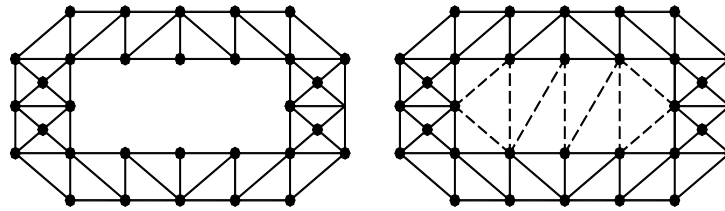
$$\gamma(S) = N_i(S) = 32.$$

The use of the classical formula (Eq. (2-2)) leads to the same result,

$$\gamma(S) = 129 - 2 \times 50 + 3 = 32,$$

but it necessitates counting 129 members and 50 nodes, compared with counting 32 internal nodes.

Example: Let S be a planar truss as shown in Figure 2.15. Triangulation of the internal region in an arbitrary manner requires 9 members, shown as dashed lines. Thus $\gamma(S) = N_i(S) - M_{ci}(S) = 16 - 9 = 7$.

(a) A planar truss S .(b) Triangulated S .**Fig. 2.15** A general planar truss and its triangulation.

Theorem 2: The DSI of a planar rigid-jointed frame S is equal to three times the number of its internal regions,

$$\gamma(S) = 3R_i(S). \quad (2-19)$$

Proof: A tree structure is statically determinate. For each addition of a chord the indeterminacy of the structure increases by 3, and therefore:

$$\gamma(S) = 3[M(S) - N(S) + 1].$$

Using Eq. (2-17) completes the proof, i.e.

$$\gamma(S) = 3R_i(S).$$

Example: The DSI of the rigid-jointed plane frame shown in Figure 2.16(a) is obtained as,

$$\gamma(S) = 3R_i(S) = 3 \times 16 = 48,$$

and for the rigid-jointed arch-type structure of Figure 2.16(b), we have:

$$\gamma(S) = 3 \times 6 = 18.$$

Obviously, the classical formula (Eq. (2-6)) requires more counting than the above method.

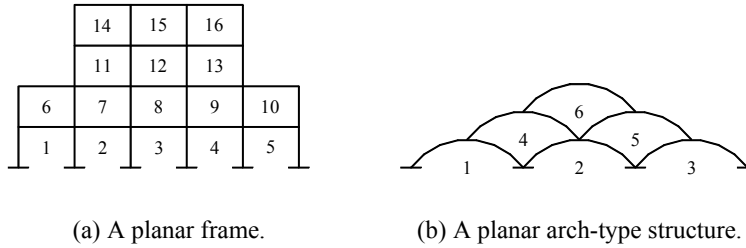


Fig. 2.16 Rigid-jointed structures.

Inter-Relation of Theorem 1 and Theorem 2: Theorem 1 and Theorem 2 are closely inter-related. Let S be a planar rigid-jointed frame and S' be a planar truss, obtained from S by introducing $[\text{deg}(n_i) - 1]$ releases in each node n_i of S , where $\text{deg}(n_i)$ is the degree of the node n_i . Then,

$$\begin{aligned}\gamma(S) &= 3M(S) - 3N(S) + 3, \\ \gamma(S') &= \gamma(S) - r, \end{aligned} \quad (2-20)$$

where r is the total number of releases given by:

$$r = \sum_{i=1}^{N(S)} [\text{deg}(n_i) - 1]. \quad (2-21)$$

Using the result of Section 1.2.2,

$$r = 2M(S) - N(S).$$

Substituting r in Eq. (2-20), and using Eq. (2-19), leads to,

$$\gamma(S') = 3[M(S) - N(S) + 1] - [2M(S) - N(S)] = M(S) - 2N(S) + 3,$$

which is the familiar classical formula for a planar truss.

Now, for a triangulated model, by Theorem 2:

$$\gamma(S) = 3R_i(S).$$

Using Eq. (2-14) leads to:

$$\gamma(S) = 2M(S) - M_e(S).$$

On the other hand,

$$\begin{aligned} \gamma(S') &= \gamma(S) - [2M(S) - N(S)] = [2M(S) - M_e(S)] - [2M(S) - N(S)] \\ &= N(S) - M_e(S) = N(S) - N_e(S) = N_i(S), \end{aligned}$$

which is the same result as that of Theorem 1.

Using a reverse process, by introducing constraints in place of releases, a truss model S' can be changed to a frame model S , and Eq. (2-19) can be derived from Eq. (2-12).

Theorem 3: A ball-jointed space truss drawn (embedded) on a sphere is internally statically determinate, if all the created regions are triangles.

Proof: Since each triangular region has three members and each member is contained in two regions, therefore:

$$3R(S) = 2M(S). \quad (2-22)$$

Combining this equation with Eq. (2-13) yields,

$$M(S) - 3N(S) + 6 = \gamma(S) = 0,$$

which completes the proof.

As an example, a ball-jointed truss with K_i of Figure 2.11(b) as its graph model, is statically determinate.

Theorem 3 can easily be generalized to graphs embedded on other surfaces such as a sphere with h handles, where Euler's formula becomes:

$$R(S) - M(S) + N(S) = 2 - 2h. \quad (2-23)$$

The substitution of Eq. (2-22) yields:

$$M(S) - 3N(S) + 6 = 6h.$$

Thus:

$$\gamma(S) = 6h.$$

As an example, the DSI of a triangulated space truss in the form of a torus (sphere with one handle), shown in Figure 2.17, becomes $\gamma(S) = 6 \times 1 = 6$.

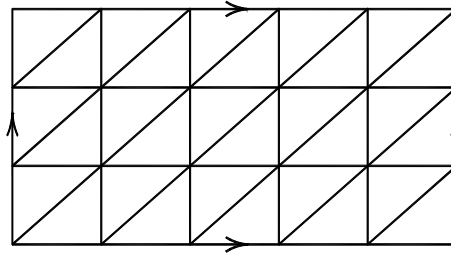


Fig. 2.17 The 1-skeleton of a triangulated torus.

2.6 SPACE STRUCTURES AND THEIR PLANAR DRAWINGS

In this section methods are developed for transforming the topological properties of space structures into those of their planar drawings, thus simplifying the counting process for the calculation of the DSI for space structures.

2.6.1 ADMISSIBLE DRAWING OF A SPACE STRUCTURE

A *drawing* S^p of a graph S in the plane is a mapping of the nodes of S to distinct points of S^p , and the members of S to open arcs of S^p such that:

- (i) the image of no member contains that of any node;
- (ii) the image of a member (n_i, n_j) joins the points corresponding to n_i and n_j .

A drawing is called *admissible (good)* if the members are such that:

- (iii) no two arcs with a common end point meet;
- (iv) no two arcs meet in more than one point;
- (v) no three arcs meet in a common point.

The configurations prohibited by these three conditions are shown in Figure 2.18.

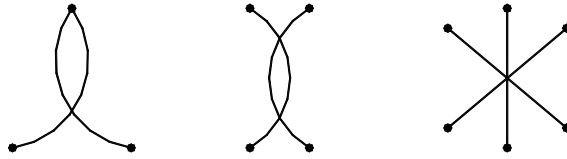
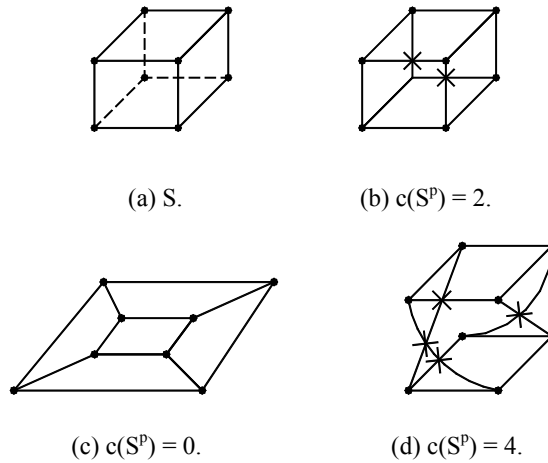


Fig. 2.18 The prohibited configurations.

A point of intersection of two members in a drawing is called a *crossing*, and the *crossing number* $c(S^p)$ of a graph S is the number of crossings in any admissible drawing of S in the plane. An *optimal* drawing in a given surface is one which exhibits the least possible crossings. In this book we will use only admissible drawings in the plane, but not necessarily optimal.

As an example, different admissible drawings of a space model, shown in Figure 2.19(a), are illustrated in Figures 2.19(b-d). The crossing points are marked by \times . The number of crossing points for each case is also provided.



(a) S .

(b) $c(S^p) = 2$.

(c) $c(S^p) = 0$.

(d) $c(S^p) = 4$.

Fig. 2.19 Admissible drawings of S .

In this example, an optimal drawing corresponds to $c(S^p) = 0$, which is shown in Figure 2.19(c).

2.6.2 THE DEGREE OF STATICAL INDETERMINACY OF FRAMES

For a rigid-jointed space frame, the DSI can be determined by using:

$$\gamma(S) = 6[M(S) - N(S) + 1]. \quad (2-24)$$

Counting the nodes in a drawing of S on the plane produces no problem, however, recognition and counting the members can be very cumbersome. The following theorem transforms this procedure to counting the crossing nodes and regions of S^p , in place of members and nodes of S .

Theorem: For a space rigid-jointed frame, the DSI is given by:

$$\gamma(S) = 6[R_i(S^p) - c(S^p)]. \quad (2-25)$$

Proof: Once a space structure is drawn in the plane, the following relationships can be established between the numbers of members and nodes of S and S^p :

$$M(S^p) = M(S) + 2c(S^p) \quad \text{and} \quad N(S^p) = N(S) + c(S^p). \quad (2-26)$$

Substituting the above equations in Eq. (2-24) yields:

$$\begin{aligned} \gamma(S) &= 6[M(S^p) - 2c(S^p) - N(S^p) + c(S^p) + 1] \\ &= 6[M(S^p) - N(S^p) + 1 - c(S^p)]. \end{aligned}$$

However, for a planar drawing:

$$M(S^p) - N(S^p) + 1 = R_i(S^p).$$

Hence:

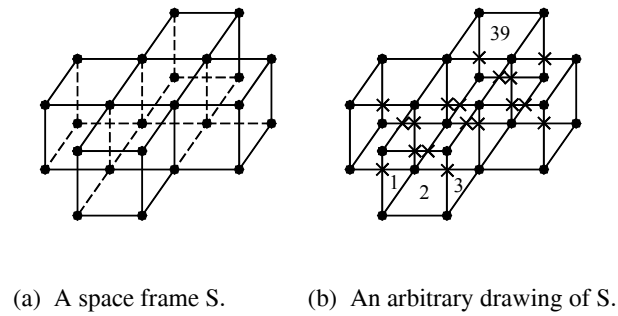
$$\gamma(S) = 6[R_i(S^p) - c(S^p)].$$

Example: In this example, S is a space frame as shown in Figure 2.20(a). An arbitrary drawing of S is illustrated in Figure 2.20(b), in which the crossing points are marked by \times . For this drawing,

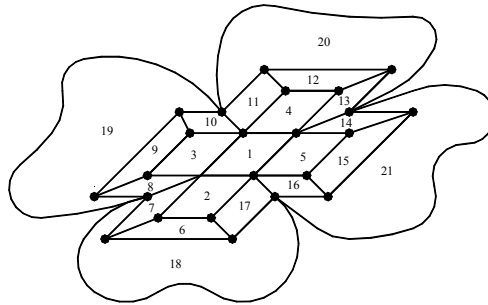
$$R_i(S^p) = 39 \quad \text{and} \quad c(S^p) = 18,$$

leading to:

$$\gamma(S) = 6[39 - 18] = 6 \times 21 = 126.$$



(a) A space frame S. (b) An arbitrary drawing of S.



(c) An optimal drawing of S.

Fig. 2.20 A space frame and its drawings.

From Eq. (2-24) one can also calculate the DSI as,

$$\gamma(S) = 6[44 - 24 + 1] = 126,$$

which requires $44 + 24 = 68$ countings in comparison to $39 + 18 = 57$ countings in the present method. This number can further be improved by constructing a drawing with a smaller number of crossings. The ideal situation corresponds to an optimal drawing. For this example, an optimal drawing is shown in Figure 2.20(c), for which,

$$R_i(S^p) = 21 \quad \text{and} \quad c(S^p) = 0,$$

leading to:

$$\gamma(S) = 6(21 - 0) = 126.$$

In this case the number of countings is reduced to 21.

Example: Let S be the graph model of a space frame as shown in Figure 2.21(a). A drawing S^p of S is shown in Figure 2.21(b) for which $c(S^p) = 8$ and $R_i(S^p) = 41$, resulting in $\gamma(S) = 6[41 - 8] = 198$.

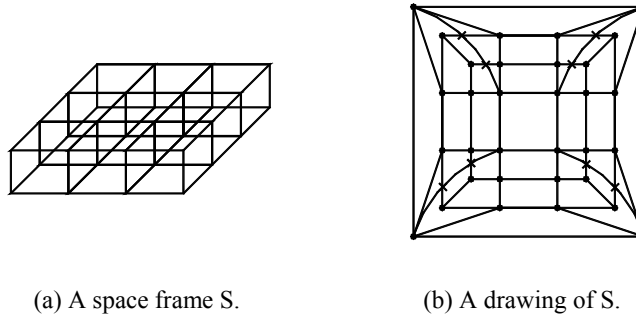


Fig. 2.21 A space frame and its drawing.

Example: Let S be the graph model of a space frame as shown in Figure 2.22(a). For an arbitrary drawing in the plane, as depicted in Figure 2.22(b),

$$c(S^p) = 12 \quad \text{and} \quad R_i(S^p) = 35.$$

Therefore: $\gamma(S) = 6[35 - 12] = 138$.

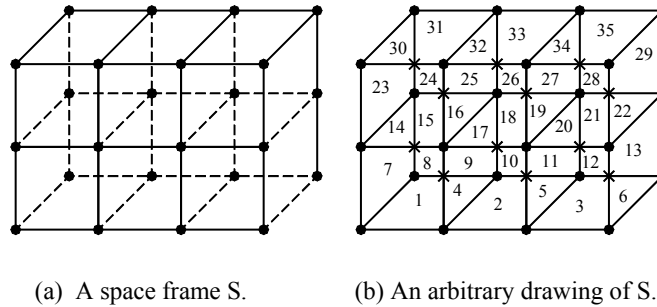


Fig. 2.22 A space frame and its planar drawings.

2.6.3 THE DEGREE OF STATICAL INDETERMINACY OF SPACE TRUSSES

Ball-jointed space trusses are often multi-member structures in the form of double and triple layer grids. The following theorem simplifies the calculation of the DSI for these structures:

Theorem: For a space ball-jointed truss supported in a statically determinate fashion, the DSI is given by,

$$\gamma(S) = c(S^p) - M_c(S^p), \quad (2-27)$$

where $c(S^p)$ is the number of crossings, and $M_c(S^p)$ is the number of members required for the full triangulation of S^p .

Proof: By adding an adequate number of members, $M_c(S^p)$, the drawing S' is obtained for which:

$$M(S') = M(S^p) + M_c(S^p) = M(S) + 2c(S^p) + M_c(S^p),$$

and

$$N(S') = N(S^p) = N(S) + c(S^p). \quad (2-28)$$

Substituting these values in the following classical formula,

$$\gamma(S) = M(S) - 3N(S) + 6,$$

leads to:

$$\begin{aligned} \gamma(S) &= M(S') - 2c(S^p) - M_c(S^p) - 3N(S') + 3c(S^p) + 6 \\ &= M(S') - 3N(S') + 6 + c(S^p) - M_c(S^p). \end{aligned}$$

By Theorem 3 of Section 2.5, for a fully triangulated graph S'^p :

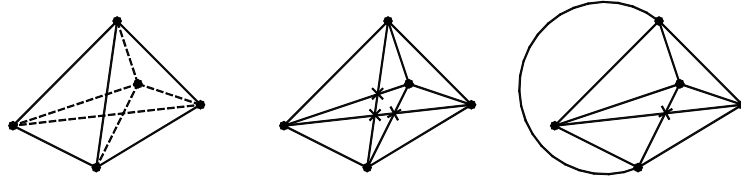
$$\gamma(S'^p) = M(S') - 3N(S') + 6 = 0.$$

Hence:

$$\gamma(S) = c(S^p) - M_c(S^p).$$

Example: S is a simple ball-jointed truss as shown in Figure 2.23(a) supported in a statically determinate fashion. An arbitrary drawing in Figure 2.23(b) has $c(S^p) = 3$ and for a full triangulation $M_c(S^p) = 2$ members are required. Therefore

$$\gamma(S) = 3 - 2 = 1.$$



(a) A space truss S. (b) An arbitrary drawing of S. (c) An optimal drawing of S.

Fig. 2.23 A space truss and two of its drawings.

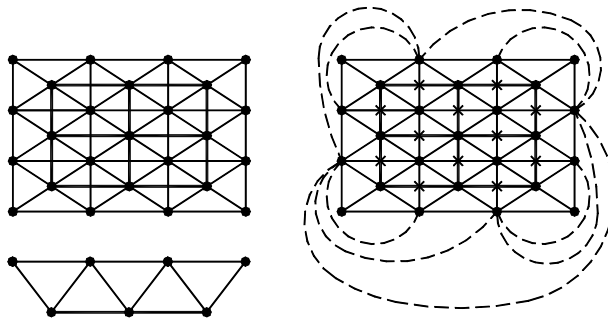
This graph is a complete graph K_5 , and according to the Kuratowski's theorem, its optimal drawing has only one crossing, as shown in Figure 2.23(c). S^p is fully triangulated and $M_c(S^p) = 0$. Therefore $\gamma(S) = 1 - 0 = 1$.

Example: Consider a space ball-jointed double layer grid S as shown in Figure 2.24(a), an admissible drawing of which is depicted in Figure 2.24(b).

This drawing contains 12 crossing points and for a full triangulation, $M_c(S^p) = 9$ members are added, as shown by dashed lines.

From Eq. (2-27) we have:

$$\gamma(S) = c(S^p) - M_c(S^p) = 12 - 9 = 3.$$



(a) A double layer grid S.

(b) An arbitrary drawing of S.

Fig. 2.24 A space truss and its planar drawings.

It should be noted that the addition of dashed lines to complete the triangulation of the exterior region (unbounded cycle) is not necessary, since an m -gone can be triangulated by $m-3$ members. Therefore one can use,

$$\gamma(S) = c(S^p) - \overline{M}_c(S^p) - m + 3, \quad (2-29)$$

where $\overline{M}_c(S^p)$ is the number of members required for a full triangulation of bounded regions.

2.6.4 COMPARISON OF CLASSICAL AND TOPOLOGICAL FORMULAE

In this section the classical and topological formulae for determining the DSI of skeletal structures are summarized as in Table 2.2. Though the classical formulae look more simple than the topological ones, the latter offer more information. Some of the advantages are as follows:

1. The number of counting for topological formulae is far less than those of the classical ones.
2. Topological formulae provide insight into the connectivity of structures and give additional information on the distribution of the indeterminacy in the vicinity of the structures.
3. The methods incorporated in the derivation of the topological formulae may be used in the study of other properties associated with graph models.

Table 2.2 Classical and topological formulae for determining the DSI.

Structural Type	Classical Formulae	Topological Formulae
Planar frame Space	$\gamma(S) = 3M(S) - 3N(S) + 3$	$\gamma(S) = 3R_i(S)$
frame Planar truss	$\gamma(S) = 6M(S) - 6N(S) + 6$	$\gamma(S) = 6[R_i(S^p) - c(S^p)]$
Space truss	$\gamma(S) = M(S) - 2N(S) + 3$	$\gamma(S) = N_i(S) - M_{ci}(S)$
	$\gamma(S) = M(S) - 3N(S) + 6$	$\gamma(S) = c(S^p) - M_c(S^p)$

In the derivation of the topological formulae it has been assumed that in each crossing point only two members cross each other. Although most of the practical structures fall into this category, the following general formulae are obtained allowing the crossing members to be more than 2 in each crossing point.

Since the derivation of the general topological formulae is similar to those of topological formulae, the proof is left as an exercise for students.

Three examples are given for illustrating the applications:

$$\text{For planar frames: } \gamma(S) = 3[R_i(S^P) - \sum_{j=2}^k (j-1)C^j(S^P)]. \quad (2-30)$$

$$\text{For space frames: } \gamma(S) = 6[R_i(S^P) - \sum_{j=2}^k (j-1)C^j(S^P)]. \quad (2-31)$$

$$\text{For planar trusses: } \gamma(S) = N_i(S^P) - M_{ci}(S^P) - \sum_{j=2}^k (j-2)C^j(S^P). \quad (2-32)$$

$$\text{For space trusses: } \gamma(S) = \sum_{j=2}^k (3-j)C^j(S^P) - M_c(S^P). \quad (2-33)$$

In the above formulae, $C^j(S^P)$ is the number of points with j members crossing at these points.

Example: A graph model S with different types of crossing points is considered as illustrated in Figure 2.25. This model contains 49 triangulated internal regions, two crossing of type C^2 , six crossings of type C^3 and one crossing of type C^4 .

When S is viewed as the model of planar truss, the DSI can be found using Eq. (2-32) as:

$$\gamma(S) = N_i(S^P) - 0 - (C^3 + 2C^4) = 14 - (6 + 2 \times 1) = 6.$$

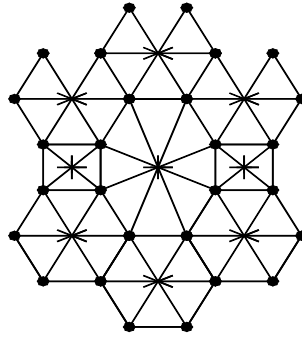


Fig. 2.25 A planar structure with different crossing point types.

For S being a planar frame, the DSI is calculated using Eq. (2-30) as:

$$\gamma(S) = 3[R_i(S^p) - (C^2 + 2C^3 + 3C^4)] = 3[49 - (2 + 2 \times 6 + 3 \times 1)] = 96.$$

Example: A graph model S with different types of crossing points is considered as illustrated in Figure 2.26. This model contains 52 internal regions, 17 internal nodes, two members are needed for triangulating the internal regions, two crossing of type C^2 , one crossings of type C^3 and one crossing of type C^4 .

When S is viewed as the model of planar truss, the DSI can be found using Eq. (2-32) as:

$$\gamma(S) = N_i(S^p) - 0 - (C^3 + 2C^4) = 17 - (2) - [(3 - 2) \times 1] + (4 - 2) \times 1 = 12.$$

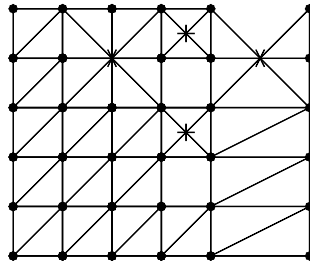


Fig. 2.26 A planar structure with different crossing point types.

For S being a planar frame, the DSI is calculated using Eq. (2-30) as:

$$\gamma(S) = 3\{52 - [(2 - 1) \times 2 + (3 - 1) \times 1 + (4 - 1) \times 1]\} = 135.$$

Using the classical formulae the same results can be obtained as:

$$\gamma(S) = 79 - 2 \times 35 + 3 = 12,$$

$$\gamma(S) = 3[79 - 35 + 1] = 135.$$

However, the number of counting for classical formulae is 114, compared to 21 and 56 for generalized topological formulae.

Example: A graph model S with two different types of crossing points is considered as illustrated in Figure 2.27. This model contains 16 internal regions, six crossing of type C^2 , one crossing of type C^3 .

When S is viewed as the model of space truss, the DSI can be found using Eq. (2-33) as:

$$\gamma(S) = 0 \times 1 + 6 - (6 + 3) = -3.$$

For S being a space frame, the DSI is calculated using Eq. (2-31) as:

$$\gamma(S) = 6[16 - 6 - 2 \times 1] = 48.$$

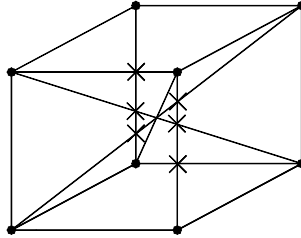


Fig. 2.27 A planar drawing of a space structure.

2.7 SUBOPTIMAL DRAWING OF A SPACE STRUCTURE

2.7.1 INTRODUCTION

For a general graph, there is no known formula by which the crossing number can be calculated. There is also no algorithm by which an optimal drawing can be obtained. The only partial results available are for special graphs like complete graphs, bipartite graphs and cubic graphs. For these graphs only upper and lower bounds for crossing numbers are available. In fact it is proven that for given graph S and an integer k , the question $c(S^p) \leq k$ is NP-complete (see Section 3.4 for the definition), Gary and Johnson [55]. Therefore, an approach for estimating crossing numbers, and the exact value of $c(S^p)$ should be restricted to special cases. As an example, for complete graphs, some results are available in Refs [43,213,246].

Two theorems of the previous subsections provide useful lower bounds for the crossing number of space structures, and lead to the design of an efficient algorithm for suboptimal drawings of a general graph.

Corollary 1: The statical indeterminacy $\gamma(S)$ of a ball-jointed space truss S , is a lower bound to the crossing number of S .

Consider Eq. (2-27) as,

$$\gamma(S) = c(S^p) - M_c(S^p),$$

and rearrange its terms as:

$$c(S^p) = \gamma(S) + M_c(S^p). \quad (2-34)$$

Since $M_c(S^p) \geq 0$, therefore:

$$c(S^p) \geq \gamma(S).$$

Hence $\gamma(S)$ is a lower bound for $c(S^p)$.

From Eq. (2-34) it follows that:

$$\text{Min } c(S^p) \leftrightarrow \text{Min } M_c(S^p). \quad (2-35)$$

Corollary 2: The crossing number of a graph is related to its Betti number by:

$$c(S^p) = R_i(S^p) - b_1(S). \quad (2-36)$$

This is obvious from Eq. (2-25) if its terms are rearranged. Therefore, to minimize $c(S^p)$ one should minimize the number of internal regions of its planar drawing, i.e.

$$\text{Min } c(S^p) \leftrightarrow \text{Min } R_i(S^p). \quad (2-37)$$

Based on the above results, an intuitive algorithm can be designed for suboptimal drawing. However, for an automatic drawing an algebraic graph theory method is developed [129] as presented in the following section.

2.7.2 AUTOMATIC DRAWING OF A SPACE STRUCTURE

Definitions: A graph can efficiently be represented by its member-node list, and the adjacency matrix of the graph can easily be constructed. Consider a graph with 10 nodes and 19 members, having the following adjacency matrix:

$$\mathbf{A} = \begin{matrix} & \begin{matrix} 1 & 2 & 3 & 4 & 5 & 6 & 7 & 8 & 9 & 10 \end{matrix} \\ \begin{matrix} 1 \\ 2 \\ 3 \\ 4 \\ 5 \\ 6 \\ 7 \\ 8 \\ 9 \\ 10 \end{matrix} & \left[\begin{array}{cccccccccc} \bullet & & & 1 & 1 & & & 1 & & \\ & \bullet & 1 & 1 & & & & & & 1 \\ & & \bullet & & & & 1 & & 1 & 1 \\ & & & \bullet & 1 & & 1 & & & \\ & & & & \bullet & & 1 & 1 & & 1 \\ & & & & & \bullet & 1 & & 1 & \\ & & & \text{sym} & & & \bullet & 1 & & 1 \\ & & & & & & & \bullet & 1 & \\ & & & & & & & & \bullet & \\ & & & & & & & & & \bullet \end{array} \right] \end{matrix}, \quad (2-38)$$

where only non-zero entries are shown for clarity. When drawing this graph, the nodes are placed on a straight line and the members are placed at the top and bottom in a random manner. Members at the top and bottom of this line are identified by +1 and -1, respectively, resulting in a new matrix \mathbf{A}^* .

For the graph shown in Figure 2.28, the corresponding matrix \mathbf{A}^* is constructed as:

$$\mathbf{A}^* = \begin{matrix} & \begin{matrix} 1 & 2 & 3 & 4 & 5 & 6 & 7 & 8 & 9 & 10 \end{matrix} \\ \begin{matrix} 1 \\ 2 \\ 3 \\ 4 \\ 5 \\ 6 \\ 7 \\ 8 \\ 9 \\ 10 \end{matrix} & \left[\begin{array}{cccccccccc} \bullet & & & -1 & -1 & & & +1 & & \\ & \bullet & +1 & -1 & & & & & & +1 \\ & & \bullet & & & & +1 & & +1 & +1 \\ & & & \bullet & +1 & & +1 & & & \\ & & & & \bullet & & -1 & -1 & & -1 \\ & & & & & \bullet & +1 & & -1 & \\ & & & & & & \bullet & +1 & & -1 \\ & & & \text{sym} & & & & & \bullet & +1 \\ & & & & & & & & & \bullet \\ & & & & & & & & & \bullet \end{array} \right] \end{matrix}. \quad (2-39)$$

For this drawing, the crossing number is equal to 8. This number can also be found from \mathbf{A}^* , using the upper triangular submatrix of \mathbf{A}^* . For a row, only the right part of the diagonal entry of that row will be considered.

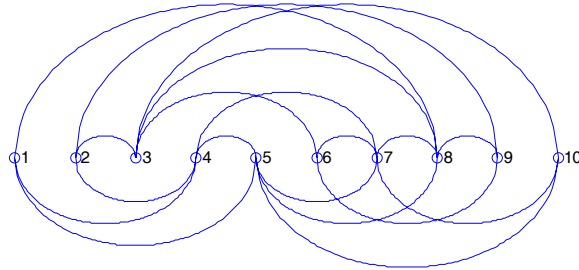


Fig. 2.28 A drawing with 8 crossings.

For each entry $\mathbf{A}^*(i,j)$ of \mathbf{A}^* , we define a subdomain of \mathbf{A}^* called the *territory* of $\mathbf{A}^*(i,j)$. This territory consists of the subdomain specified by $\mathbf{A}^*(1:i-1, i+1:j-1)$, denoted by $\text{SUBA}^*(1:i-1, i+1:j-1)$. The territory corresponding to the (i,j) th entry contains the entries from row 1 to $i-1$, and column $i+1$ to $j-1$. As an example, the region corresponding to $(3,10)$ th entry of \mathbf{A}^* contains the entries confined to rows 1 to 2 and columns 4 to 9, i.e. for $\mathbf{A}^*(3,10)$ the territory is shown by $\text{SUBA}^*(1:2, 4:9)$.

For each subdomain there is an associated crossing number, which is the same as the number of entries having the same sign as the considered entry. As an example, for the entry $(3,10)$ shown in \mathbf{A}^* , the number of +1s is equal to 2. Obviously if $\mathbf{A}^*(3,10)$ was -1 , then the number of crossings would be equal to 3.

For all non-zero entries of \mathbf{A}^* , the territory can be specified and their crossing numbers can be calculated and summed up, resulting in the number of crossings of the drawing. In the above example, the member connecting 3 to 10 have crossing points with the members 1 to 8 and 2 to 9, since in this territory, both members are drawn at the top.

Present Method: For a fixed positioning of the nodes on a straight line, the number of members (entries) is constant, however, the number of crossings should be minimized [27,123]. This can be achieved by reducing the crossing numbers of the territories. As an example, in matrix \mathbf{A}^* , the entries $(2,9)$ and $(1,8)$ can be changed to -1 , however, this may have a reverse effect on the number of crossings of the other territories, hence increasing the number of crossings of the drawing.

Now we associate consecutive numbers with each non-zero entry of \mathbf{A}^* , to obtain matrix \mathbf{B} as follows:

$$\mathbf{B} = \begin{matrix} & \begin{matrix} 1 & 2 & 3 & 4 & 5 & 6 & 7 & 8 & 9 & 10 \end{matrix} \\ \begin{matrix} 1 \\ 2 \\ 3 \\ 4 \\ 5 \\ 6 \\ 7 \\ 8 \\ 9 \\ 10 \end{matrix} & \left[\begin{array}{cccccccccc} \bullet & & & 1 & 2 & & & 3 & & \\ & \bullet & 4 & 5 & & & & & 6 & \\ & & \bullet & & & & 7 & 8 & 9 & \\ & & & \bullet & 10 & & 11 & & & \\ & & & & \bullet & & 12 & 13 & & 14 \\ & & & & & \bullet & 15 & & 16 & \\ & & & & & & \bullet & 17 & & 18 \\ & & \text{sym} & & & & & \bullet & 19 & \\ & & & & & & & & \bullet & \\ & & & & & & & & & \bullet \end{array} \right] \end{matrix} \quad (2-40)$$

The numbers 1 to 19 are associated with these entries for 19 members. For the previous example, the territory of node 9 will contain numbers 1,2,3,5 and 6. Now we define a virtual graph whose nodes are the same as the number of members of the original graph and two nodes n_i and n_j are connected if n_j is in the subdomain of n_i . For the considered graph, the node 9 is connected to the nodes 1,2,3,5 and 6. Other members are formed considering the other territories.

Since two types of numbers are used in the territory, i.e. +1 and -1, the members can be identified using two colours. Obviously for the virtual graph G_v , if a member has two nodes of the same colour, this will be equivalent to a crossing.

Now an optimal planar drawing (embedding) can be constructed as follows:

Colour the nodes of G_v in such a manner that no two adjacent nodes have the same colour. Obviously this is possible only if 4 colours are available (Ref. [183]). However, if a graph can be coloured with two colours only, it is equivalent to a planar drawing with no crossing. It can be shown that only bipartite graphs with no odd cycles are two-colourable. However, if a graph is not two-colourable, at least one should reduce the number of members with the nodes of the same colour. This is equivalent to having a pseudo-bipartite graph, each part of which contains a limited number of members. Using the adjacency matrix \mathbf{A}_v of G_v , one can decompose the graph into two subgraphs with close properties to a bipartite graph, i.e. two subgraphs with maximal interface.

Methods for bisection with minimum interface use the Fiedler vector of the Laplacian of a graph [101,218]. The connection between two subgraphs can be represented as $C = \frac{1}{8} \mathbf{x}^t \mathbf{L} \mathbf{x}$ using Rayleigh's minimal principle. Minimal C corresponds to λ_2 of \mathbf{L} , since $\lambda_1=0$, and λ_n corresponds to maximal C . It should be noted that for some graphs, λ_3 produces better results than λ_2 , and similarly in

It can be seen that the matrix in Figure 2.30 is not well structured, however, the corresponding crossing number has the least magnitude.

Examples: For complete graphs, all the entries are present in \mathbf{A} , and therefore the least crossing can be evaluated much easier. The present algorithm is applied to K_{10} , K_{13} , and K_{15} , and corresponding graphs are drawn in Figures 2.31 to 2.33. The number of crossings, satisfies the following known inequality:

$$v(K_n) \leq \frac{1}{4} \left[\frac{n}{2} \right] \left[\frac{n-1}{2} \right] \left[\frac{n-2}{2} \right] \left[\frac{n-3}{2} \right], \quad (2-43)$$

where $v(K_n)$ is the crossing number and K_n is a complete graph containing n nodes [68].

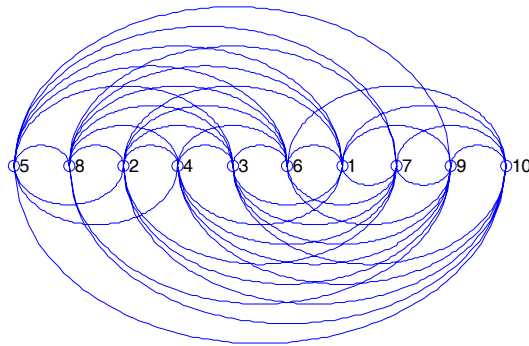


Fig. 2.31 A planar drawing of K_{10} .

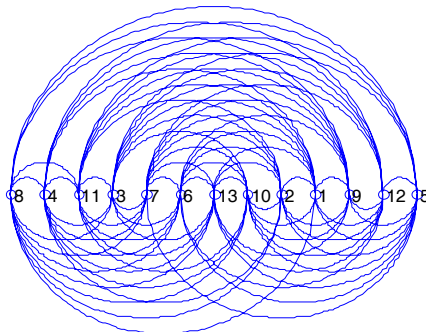


Fig. 2.32 A planar drawing of K_{13} .

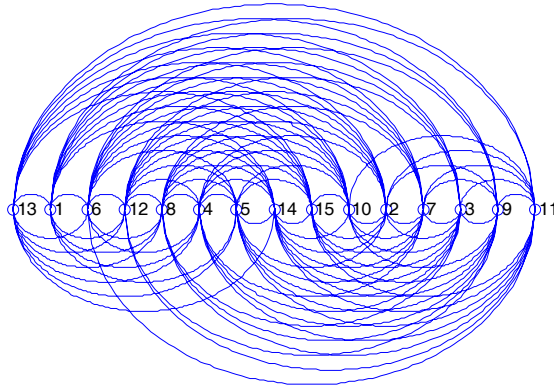


Fig. 2.33 A planar drawing of K_{15} .

As mentioned before, for the above examples no trial and error method is used to improve the positioning; and the present approach is merely employed. There is no general method for such positioning, and one can use a greedy type algorithm, although there is no guarantee in obtaining minimal crossings, which is an NP-complete problem [55].

For structural models, the ratio of the numbers of members to the number of nodes, is far less than those of complete graphs. For such models, one can decompose the models into an appropriate number of subgraphs having minimal interfaces; for each subgraph the embedding can be performed separately.

In the following, two examples of structural models are studied. The planar drawing of the space frame in Figure 2.21 is illustrated in Figure 2.34. The planar embedding of the double layer grid shown in Figure 2.24 is provided in Figure 2.35.

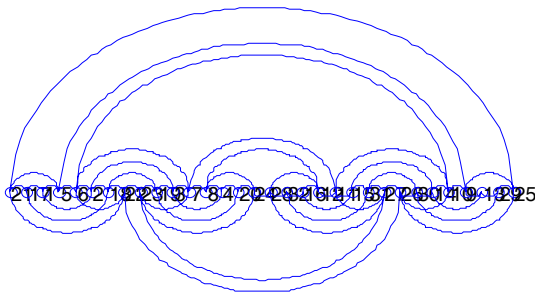


Fig. 2.34 A planar drawing of the space frame with 8 crossings.

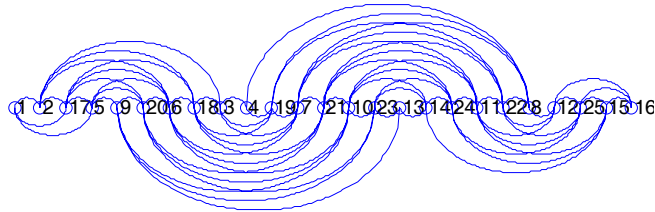
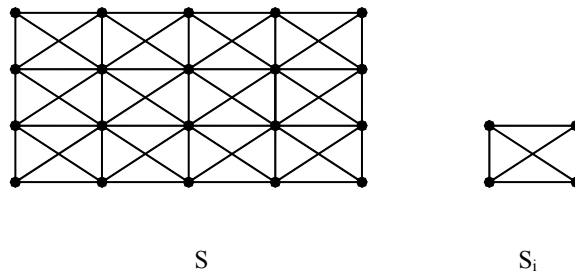


Fig. 2.35 A planar drawing of the space frame with 12 crossings.

The application of the present method is by no means confined to finding the DSI of structures. It can be extended to other systems such as electrical and hydraulic systems, printed circuit board layout, very large-scale integration circuit routing and automated graph drawing.

EXERCISES

2.1 Use an expansion process to find the DSI of a 3×4 planar truss S as shown. The unit to be considered for expansion is also given.



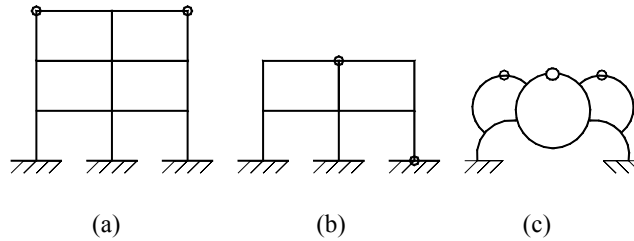
2.2 If the truss in the previous example is an $m \times n$ planar truss, determine the corresponding DSI.

2.3 Find the DKI of the truss in Exercise 2.1 and compare it with its DSI. What do you conclude?

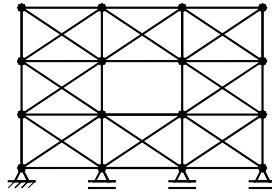
2.4 Derive Eq. (2-9) from Eq. (2-8).

2.5 Prove that for determining the DSI of a planar truss, the crossing point of any two members can be regarded as an extra node. If the crossing members are more than two, why does such an operation become incorrect?

2.6 Determine the DKI and the DSI of the following planar frames with some releases:



2.7 Find the DSI of the following planar truss using three different methods: classical, modification and triangulation:



2.8 Determine the DSI of S_1 in Figure 2.9 using its planar drawing. Consider S_1 first as a space truss and secondly as a space frame.

2.9 Determine the DSI of the following double-layer grid. Suppose S is supported in a statically determinate fashion.

